

# Review on Sustainable Approaches in Nanotechnology: Green Synthesis, Characterization and Application of Hematite Nanoparticles ( $\alpha$ -Fe<sub>2</sub>O<sub>3</sub> NPs)

Dave Hardika<sup>1</sup>, Madhuresh Makavana<sup>2</sup>, Keyur Bhatt<sup>3</sup>

<sup>1</sup>Research scholar, Chemistry, Ganpat University

<sup>2</sup>Scientific Officer, Regional Forensic Science laboratory

<sup>3</sup>Associate professor, Chemistry, Ganpat University

## Abstract:

Hematite ( $\alpha$ -Fe<sub>2</sub>O<sub>3</sub>) nanoparticles (NPs) have garnered significant attention as an environmentally benign nanomaterial with diverse applications in environmental remediation and biological systems. This review critically examines the green synthesis methodologies, physicochemical properties, and multifaceted applications of  $\alpha$ -Fe<sub>2</sub>O<sub>3</sub> NPs. Green synthesis protocols utilizing plant extracts as both reducing and stabilizing agents have been extensively explored, yielding  $\alpha$ -Fe<sub>2</sub>O<sub>3</sub> NPs with diameters ranging from 1 to 100 nm. These biogenic synthesis routes offer advantages in terms of eco-compatibility, cost-effectiveness, and scalability compared to conventional chemical methods. Characterization studies reveal that green-synthesized  $\alpha$ -Fe<sub>2</sub>O<sub>3</sub> NPs exhibit notable antimicrobial efficacy against both Gram-positive and Gram-negative bacterial strains. Additionally, these nanoparticles demonstrate enhanced photocatalytic activity under both solar irradiation and dark conditions, attributed to their unique surface properties and electronic structure. The review highlights the potential of  $\alpha$ -Fe<sub>2</sub>O<sub>3</sub> NPs in wastewater treatment applications, particularly their role as heterogeneous catalysts for the degradation of organic dyes at neutral pH. The synergistic effects of their adsorptive capacity and catalytic activity contribute to efficient pollutant removal. Green-synthesized  $\alpha$ -Fe<sub>2</sub>O<sub>3</sub> NPs present a promising platform for addressing environmental challenges, combining eco-friendliness with high efficiency. Future research directions should focus on elucidating the mechanisms of nanoparticle formation, optimizing synthesis parameters for enhanced performance, and evaluating the long-term environmental impact of these nanomaterials.

**Keywords:** Hematite nanoparticles, green synthesis, wastewater treatment, Photocatalysis, antimicrobial activity, environmental remediation

## 1. Introduction

Nanotechnology has come out as a transformative field with far-reaching implications across diverse scientific disciplines, including biomedical engineering, surface science, environmental science, and applied physics. The synthesis and application of nanoscale materials, particularly those with size ranging from 1 to 100 nm have garnered significant attention due to their unique physicochemical properties such as enhanced conductivity, high surface to volume ratios, and exceptional catalytic activity[1], [2].

While conventional physical and chemical methods (e.g., sol gel, chemical reduction, co-precipitation, and hydrothermal synthesis) have been widely employed for nanoparticle (NP) synthesis, these approaches often involve the use of toxic chemicals, raising concerns about their environmental impact [3]. Consequently, there has been a paradigm shift towards eco-friendly "green" synthesis methodologies, utilizing extracts from plant parts, fruits, and vegetables as reducing and stabilizing agents [4].

Environmental pollution, particularly water contamination, presents a critical global challenge. The discharge of inadequately treated wastewater containing harmful substances such as dyes, pharmaceuticals, and personal care products poses significant risks to human health and ecosystem integrity [5], [6]. According to the 2022 UN Sustainable Development Goals report, while progress has been made in wastewater treatment, with 76% of wastewater receiving at least secondary treatment in 73 countries, water quality degradation remains a pressing concern [7]. The textile industry, for instance, contributes approximately one-fifth of global water pollution, highlighting the urgent need for effective remediation strategies [8].

Among various nanomaterials, iron oxide nanoparticles, particularly hematite ( $\alpha$ -Fe<sub>2</sub>O<sub>3</sub>), have garnered considerable interest due to their unique characteristics such as low toxicity, high adsorption capacity, surface reactivity, magnetic properties, and catalytic efficiency [9]. The ability to modulate the size, shape, and morphology of  $\alpha$ -Fe<sub>2</sub>O<sub>3</sub> NPs allows for the fine-tuning of their optical, magnetic, and electrical properties, enhancing their charge transfer capabilities and making them particularly suitable for green synthesis approaches [10].

In the biomedical domain,  $\alpha$ -Fe<sub>2</sub>O<sub>3</sub> NPs have shown promise in addressing complex challenges such as cancer therapeutics and combating antibiotic-resistant bacteria [11], [12]. The structural stability of  $\alpha$ -Fe<sub>2</sub>O<sub>3</sub> NPs under atmospheric conditions, coupled with their therapeutic and antibacterial properties, positions them as versatile candidates for biological applications [13].

## 2. Green synthesis of $\alpha$ -Fe<sub>2</sub>O<sub>3</sub> NPs from plant extracts:

Conventional physical and chemical methods for synthesizing  $\alpha$ -Fe<sub>2</sub>O<sub>3</sub> nanoparticles (NPs) often require high energy inputs, substantial space, and costly equipment [14]. In contrast, green synthesis approaches utilize biological organisms such as plants, bacteria, fungi, algae, and actinomycetes offer eco-friendly and cost-effective alternatives [12], [14]. While microbial-based synthesis presents certain advantages, it also poses challenges related to toxicity and stringent biosafety requirements [15].

Plant-mediated synthesis of  $\alpha$ -Fe<sub>2</sub>O<sub>3</sub> NPs has garnered significant attention owing to the presence of phytochemicals in plant extracts [16]. These bioactive compounds, including phenolic acids, terpenoids, flavonoids, and alkaloids, serve as effective reducing and stabilizing agents owing to their specific functional group (Figure: 1), which are found in plants extracts. So, plants extracts are highly effective for synthesis of  $\alpha$ -Fe<sub>2</sub>O<sub>3</sub> NPs [16], [17].

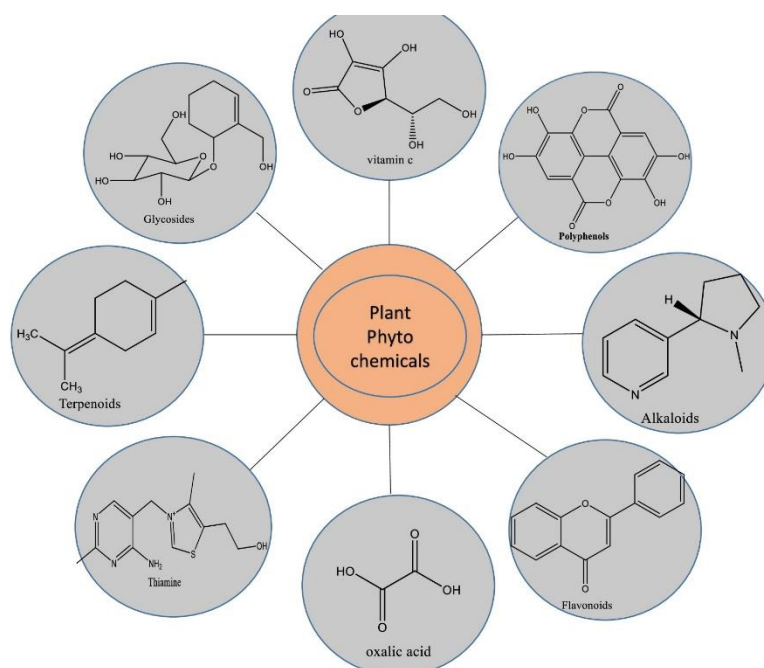


**Figure: 1 Plant Phytochemicals[17]**

Electron rich biomolecules containing hydroxyl groups (-OH) can efficiently reduce iron ions from divalent ( $\text{Fe}^{2+}$ ) or trivalent ( $\text{Fe}^{3+}$ ) oxidation states to  $\text{Fe}^0$  depending on the iron precursor used [18]. The properties of the synthesized NPs are primarily determined by factors such as type and concentration of plant extract, volume ratio of extract to metal salt solution, reaction parameters (pH, temperature, incubation period [19].

The typical process for green synthesis of  $\alpha\text{-Fe}_2\text{O}_3$  NPs using plant extracts involves:

1. Collection and preparation of plant material: Washing with distilled water to remove impurities, Drying at room temperature and Grinding into fine powder using appropriate equipment (e.g., mortar and pestle, blender, Wiley mill, or electric grinder)[16], [19].
2. Extraction of bioactive compounds: Mixing plant powder with suitable solvents (e.g., water, methanol, ethanol), Heating and stirring the mixture to facilitate extraction[20].
3. Nanoparticle synthesis: Addition of plant extract to an appropriate iron precursor solution, Observation of colour changes indicative of NPs formation, which vary depending on the salt employed[16], [20], [21]

Researcher have successfully synthesized  $\alpha\text{-Fe}_2\text{O}_3$  NPs using extracts from various plant species, including Teucrium Polium[22], Piper Betel[23], Oscillatoria limnetica[24], Rosmarinus Officinalis[25], Tamarix Aphylla[26] etc.

### 3. Optimization

The morphological characteristics and yield optimization of green-synthesized  $\alpha\text{-Fe}_2\text{O}_3$  nanoparticles (NPs) are critically dependent on several key parameters, including temperature, pH, precursor type, and precursor concentration [27].

#### 3.1 Effect of Temperature

Temperature plays a pivotal role in the green synthesis of  $\alpha\text{-Fe}_2\text{O}_3$  NPs ranging from  $25^\circ\text{C}$  to  $100^\circ\text{C}$ . The selection of an appropriate temperature is crucial due to the following factors:

1. **Phytochemical stability:** Many plant secondary metabolites serve as reducing and capping agents are thermolabile. Consequently, numerous research groups select room temperature synthesis to preserve the integrity of these bioactive compounds.
2. **Reaction kinetics:** Temperature significantly influences the reaction rate and, by extension, the morphology of the resultant NPs. Higher reaction temperatures have been observed to alter NP morphology, potentially due to increased molecular motion and collision frequency [28].
3. **Synthesis time:** UV-Visible spectroscopic analysis has indicate that the complete formation of iron oxide NPs from plant extracts occurs within 48 hours at 30°C and 72 hours at 40°C[29]. This temperature-dependent reaction time highlights the kinetic aspects of NP formation.
4. **Size control:** A study utilizing *Rheum emodi* root extract reported the successful synthesis of  $\alpha$ -Fe<sub>2</sub>O<sub>3</sub> NPs with an average diameter of ~12 nm at 60°C[30]. This finding suggests that moderate temperature elevation can be employed for size-controlled synthesis while maintaining the benefits of the green approach.

The optimization of temperature in green synthesis protocols for  $\alpha$ -Fe<sub>2</sub>O<sub>3</sub> NPs requires careful consideration of the balance between reaction efficiency, desired NP characteristics, and the preservation of bioactive plant compounds. Further research warranted to elucidate the precise mechanisms by which temperature influences NP formation and properties in plant-mediated synthesis

### 3.2 Effect of pH

The pH of the reaction medium is a critical optimization parameter influencing the green synthesis of NPs from various plant extracts [27]. The size and morphology of NPs are significantly affected by variations in the solution pH [31]. In a study, on the green synthesis of  $\alpha$ -Fe<sub>2</sub>O<sub>3</sub> NPs, it is observed that the formation rate of NPs began to decrease at pH > 9 and was completely inhibited at pH values of 12.0 or 4.0. This indicated that a pH below 10 was optimal for the rapid synthesis of  $\alpha$ -Fe<sub>2</sub>O<sub>3</sub> NPs, with the ideal pH range determined to be 8–10 [29]. An investigation into the green synthesis of iron oxide NPs using *Phoenix dactylifera L.* (date palm) extract demonstrated clear pH-dependent effects on the resulting magnetic iron oxide nanoparticles [32]. The study revealed that biosynthesis was entirely suppressed at both highly alkaline (pH 12) and acidic (pH 4) conditions. These findings suggest that extreme pH environments, whether highly basic or acidic, are unfavourable for the utilization of plant extracts in the synthesis of iron oxide nanoparticles (IONPs) [27].

### 3.3 Effect of precursor and concentration of precursor

A variety of iron-containing precursors have been employed in the green synthesis of  $\alpha$ -Fe<sub>2</sub>O<sub>3</sub> NPs using plant extracts. [27]. These precursors include ferric nitrate, ferric chloride, iron acetate, ferrous sulphate, ferric citrate and ammonium ferric citrate. Previous studies have demonstrated that the choice of precursor significantly influences the reaction kinetics, as well as the morphology and dimensions of the resultant nanoparticles. [29]. This influence is attributed to variations in the precursors' shape, size, and aqueous solubility.

Furthermore, research has shown that the concentration of the precursor plays a crucial role in determining both the synthesis duration of iron oxide nanoparticles (IONPs) and their final particle size distribution. These findings underscore the importance of carefully selecting and optimizing precursor type and concentration to achieve desired nanoparticle characteristics and synthesis efficiency in green synthesis protocols.

#### 4. Characterization Techniques

Characterization techniques are utilized to elucidate the chemical, physical, mechanical, and electrical properties of newly synthesized particles.

##### 4.1 UV-Visible spectroscopic technique:

UV-Visible spectroscopy is a crucial analytical tool for characterizing green-synthesized  $\alpha$ -Fe<sub>2</sub>O<sub>3</sub> NPs, providing confirmation of their formation and insights into their optical properties. In this technique, a beam of light is transmitted through the sample solution, and the absorbance is measured across a spectrum of wavelengths [33]. For  $\alpha$ -Fe<sub>2</sub>O<sub>3</sub> NPs, characteristic absorption peaks typically manifest within the 200-800 nm range, with specific peaks often observed between 230 and 290 nm. These spectral features serve as indicators of successful synthesis and provide information about particle characteristics [34], [35]. In a study involving  $\alpha$ -Fe<sub>2</sub>O<sub>3</sub> NPs synthesized from *Cyperus rotundus L.*, researchers observed a strong absorption band in the visible range, accompanied by minor spectral features in the UV range, using an Optizen 3220 double beam UV-Vis spectrophotometer [36]. Another investigation, focusing on the formation of  $\alpha$ -Fe<sub>2</sub>O<sub>3</sub> NPs from *Rheum emodi*, reported surface plasmon resonance (SPR) peaks at 270 nm and 320 nm in the UV-visible spectrum. These spectral features were interpreted as evidence for the synthesis of  $\alpha$ -Fe<sub>2</sub>O<sub>3</sub> NPs capped with hydroxy-antraquinones [30]. These studies demonstrate the utility of UV-Visible spectroscopy in confirming nanoparticle synthesis and providing preliminary insights into their optical properties and surface chemistry.

##### 4.2 Fourier-Transform Infrared (FT-IR) Spectroscopic Analysis

Fourier-Transform Infrared (FT-IR) spectroscopy has been employed to characterize green-synthesized hematite ( $\alpha$ -Fe<sub>2</sub>O<sub>3</sub>) nanoparticles presented in Figure:2 (a) [23], [37].

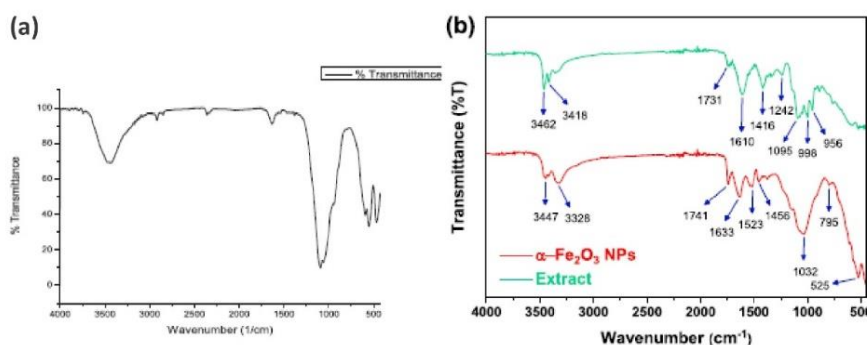


**Figure:2 (a) FT-IR spectrum of  $\alpha$ -Fe<sub>2</sub>O<sub>3</sub>NPs<sup>1</sup>[23] (b) FT-IR spectrum of Fe<sub>2</sub>O<sub>3</sub>NPs<sup>2</sup> [38]**

In a study by Adeel Ahmed et al., FT-IR analysis was conducted on  $\alpha$ -Fe<sub>2</sub>O<sub>3</sub> NPs synthesized using *Punica granatum* seed extract. The resulting spectrum, shown in Figure: 2 (b), revealed absorption bands at 3447,

<sup>1</sup>Reprinted from Science Direct, *Mater. Today Proc.*, vol. 46, J. Yoonus, R. Resmi, and B. Beena, "Evaluation of antibacterial and anticancer activity of green synthesized iron oxide ( $\alpha$ -Fe<sub>2</sub>O<sub>3</sub>) nanoparticles," no. 03, pp. 2969–2974, 2020, with permission from Elsevier doi: [10.1016/j.matpr.2020.12.426](https://doi.org/10.1016/j.matpr.2020.12.426).

<sup>2</sup>Reprinted from Science Direct, *J. Mol. Liq.*, vol. 339, A. Ahmed, M. Usman, B. Yu, Y. Shen, and H. Cong, "Sustainable fabrication of hematite ( $\alpha$ -Fe<sub>2</sub>O<sub>3</sub>) nanoparticles using biomolecules of *Punica granatum* seed extract for unconventional solar-light-driven photocatalytic remediation of organic dyes," p. 116729, 2021, with permission from Elsevier doi: [10.1016/j.molliq.2021.116729](https://doi.org/10.1016/j.molliq.2021.116729).

3328, 1741, 1633, 1523, 1456, 1032, 795, and 525  $\text{cm}^{-1}$ . The peaks observed at 3447 and 3328  $\text{cm}^{-1}$  were attributed to O-H stretching vibrations, likely originating from polyphenols bound to the surface of the  $\alpha\text{-Fe}_2\text{O}_3$  NPs. Notably, the spectral region between 500-1000  $\text{cm}^{-1}$  exhibited peaks predominantly associated with metal-oxygen bonding, providing evidence for the successful synthesis of  $\alpha\text{-Fe}_2\text{O}_3$  NPs. The characteristic band at 525  $\text{cm}^{-1}$ , which corresponds to the Fe-O stretching vibrations within the  $\alpha\text{-Fe}_2\text{O}_3$  NPs. The presence of this band further corroborates the formation of the desired nanoparticles [38]. This FT-IR analysis not only confirms the synthesis of  $\alpha\text{-Fe}_2\text{O}_3$  NPs but also provides insights into the surface chemistry and potential interactions between the nanoparticles and the biomolecules derived from the plant extract used in their green synthesis.

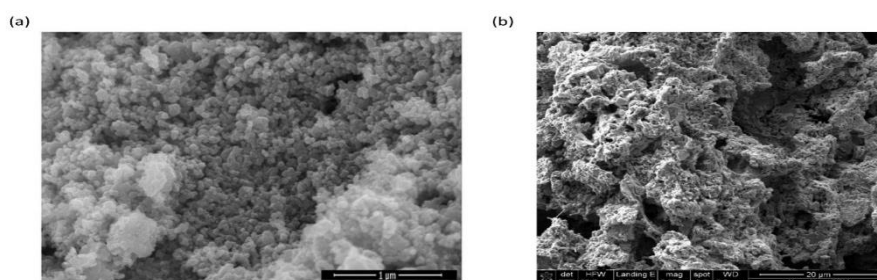
#### 4.3 Scanning Electron Microscopy (SEM) and Field Emission Scanning Electron Microscopy (FE-SEM) Analysis

Scanning Electron Microscopy (SEM) and Field Emission Scanning Electron Microscopy (FE-SEM) are powerful techniques for characterizing nanoparticle morphology and size distribution. The primary distinction between these methods lies in their electron source: SEM utilizes thermionic emitters, while FE-SEM employs field emitters or electron guns, offering enhanced resolution and image quality. [39]. SEM analysis was employed to elucidate the morphology and shape of green-synthesized  $\alpha\text{-Fe}_2\text{O}_3$  NPs derived from *Oscillatoria limnetica*, as illustrated in Figure 3(a) [24]. This technique provided valuable insights into the nanoparticle structure at the microscale level.

In a separate study conducted by S.K. Noukelag et al., FE-SEM analysis was performed on  $\alpha\text{-Fe}_2\text{O}_3$  NPs synthesized using *Rosmarinus officinalis* leaves. The nanoparticles were subjected to an annealing process at 500°C for 2 hours prior to imaging using a Zeiss Ultra 55 Scanning Electron Microscope. Particle size distribution was assessed by fitting histogram data to a Gaussian distribution. The results revealed an average particle size of  $6.531 \pm 0.148$  nm, as depicted in Figure 3(b)[25]. This high-resolution analysis allowed for precise determination of nanoparticle dimensions and morphological characteristics.

These SEM and FE-SEM analyses of  $\alpha\text{-Fe}_2\text{O}_3$  NPs demonstrate that eco-friendly synthesis methods can produce nanoparticles with well-defined morphologies and controlled size distributions. Such detailed characterization is crucial for understanding the relationship between synthesis parameters and the resulting nanoparticle properties, ultimately informing the optimization of green synthesis protocols for  $\alpha\text{-Fe}_2\text{O}_3$  NPs with tailored characteristics.

**Figure: 3(a) SEM image of *Oscillatoria limnetica*-mediated IONPs<sup>3</sup>[24]. (b) FESEM image of  $\alpha\text{-Fe}_2\text{O}_3$  NPs from *Rosmarinus officinalis* leaves<sup>4</sup> [25]**



<sup>3</sup> Reprinted from MDPI, *Molecules*, vol. 28, M. Haris et al., “*Oscillatoria limnetica* Mediated Green Synthesis of Iron Oxide ( $\text{Fe}_2\text{O}_3$ ) Nanoparticles and Their Diverse In Vitro Bioactivities,” no. 5, 2023, doi: [10.3390/molecules28052091](https://doi.org/10.3390/molecules28052091)

<sup>4</sup> Reprinted from Science Direct, *Today Proc.*, vol. 43, S. K. Noukelag, C. J. Arendse, and M. Maaza, “Biosynthesis of hematite phase  $\alpha\text{-Fe}_2\text{O}_3$  nanoparticles using an aqueous extract of *Rosmarinus officinalis* leaves”, pp. 3679–3683, 2020, with permission from Elsevier, [10.1016/j.matpr.2020.10.977](https://doi.org/10.1016/j.matpr.2020.10.977).

#### 4.3.1 Energy-Dispersive X-ray Spectroscopy (EDX) Analysis

Energy-Dispersive X-ray Spectroscopy (EDX) often coupled with Scanning Electron Microscopy (SEM), is a powerful analytical technique used to determine the elemental composition of nanoparticles.[40]. This method has been extensively applied to characterize green-synthesized  $\alpha$ -Fe<sub>2</sub>O<sub>3</sub> nanoparticles (NPs). In a study utilizing *Rhus punjabensis* for  $\alpha$ -Fe<sub>2</sub>O<sub>3</sub> NP synthesis, EDX analysis confirmed the presence and relative abundance of Fe and O in nanoparticles [41]. Another investigation employing a precipitation method reported EDX results indicating 27.34% iron and 68% oxygen content in the synthesized  $\alpha$ -Fe<sub>2</sub>O<sub>3</sub> NPs, demonstrating the technique's utility in quantifying elemental composition [42]. EDX analysis of  $\alpha$ -Fe<sub>2</sub>O<sub>3</sub> NPs using *Sida cordifolia* plant extract revealed an elemental composition of approximately 39.37% iron and 60.63% oxygen. These proportions suggested high purity of the synthesized nanoparticles [43]. EL-KASSAS Hala et al. conducted an EDX investigation on iron oxide nanoparticles synthesized via green chemistry methods using two distinct seaweeds. Their analysis identified a characteristic peak for iron at a binding energy of 6.39 keV, as illustrated in Figure 4 [44]. Typically, EDX spectra of  $\alpha$ -Fe<sub>2</sub>O<sub>3</sub> NPs exhibit strong peaks for iron and oxygen without significant impurity signals, indicating high purity [34].]. The atomic ratio of iron to oxygen often approximates 2:3, consistent with the stoichiometry expected for the hematite crystal structure [45]. EDX analysis has proven to be an invaluable tool for verifying the elemental composition and purity of  $\alpha$ -Fe<sub>2</sub>O<sub>3</sub> NPs produced through green synthesis methods, particularly those utilizing plant extracts as reducing and capping agents. This technique provides crucial information about the chemical nature of the synthesized nanoparticles, complementing other characterization methods and supporting the efficacy of eco-friendly synthesis protocols.

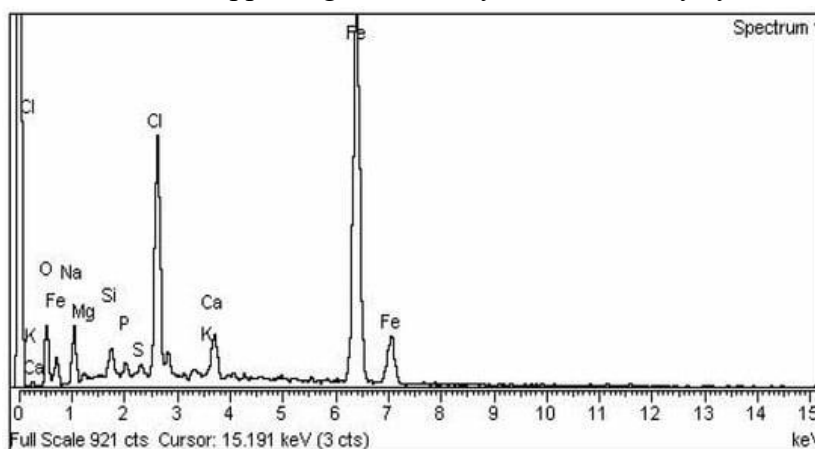


**Figure: 4 EDX spectra of  $\alpha$ -Fe<sub>2</sub>O<sub>3</sub>NPs synthesized using *Oscillatoria limnetica*<sup>5</sup> [24]**

#### 4.4 X-Ray Diffraction (XRD) Analysis

X-ray diffraction (XRD) is a powerful analytical technique employed to characterize the crystalline nature and phase purity of  $\alpha$ -Fe<sub>2</sub>O<sub>3</sub> nanoparticles (NPs). This method utilizes X-rays, a form of electromagnetic radiation with wavelengths comparable to interatomic spacings in crystalline solids, enabling the determination of crystal domain size and structural properties of nanomaterials[46]. XRD analysis of  $\alpha$ -Fe<sub>2</sub>O<sub>3</sub> NPs synthesized using *Hibiscus* extract revealed polycrystalline characteristics with average crystallite sizes of approximately 20 nm. The hematite phase was confirmed through the identification of specific diffraction peaks at characteristic  $2\theta$  values in the XRD pattern [47]. In a similar study,  $\alpha$ -Fe<sub>2</sub>O<sub>3</sub>

<sup>5</sup> Reprinted from MDPI, *Molecules*, vol. 28, M. Haris *et al.*, “*Oscillatoria limnetica* Mediated Green Synthesis of Iron Oxide (Fe<sub>2</sub>O<sub>3</sub>) Nanoparticles and Their Diverse In Vitro Bioactivities,” , no. 5, 2023, doi: [10.3390/molecules28052091](https://doi.org/10.3390/molecules28052091).

NPs with an average particle size of about 18 nm were reported, with diffraction peaks indexed to the hematite crystal structure, indicating successful synthesis and crystallinity [45].

Figure 5 presents the XRD patterns of  $\alpha$ -Fe<sub>2</sub>O<sub>3</sub> NPs synthesized using *Mentha pulegium* extract. The multiple well-defined peaks in the XRD pattern indicated the formation of crystalline nanoparticles. Specifically, diffraction peaks were observed at 2 $\theta$  angles of 30.28°, 35.20°, 43.68°, 54.01°, 57.55°, and 63.36°, corresponding to the crystallographic planes (220), (311), (400), (422), (511), and (440), respectively [48]. These findings highlight the effectiveness of green synthesis methods in producing well-defined  $\alpha$ -Fe<sub>2</sub>O<sub>3</sub>NPs.

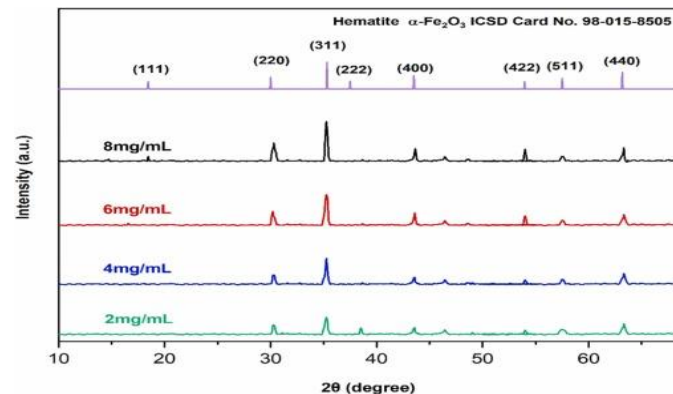


**Figure: 5 XRD spectra of  $\alpha$ -Fe<sub>2</sub>O<sub>3</sub> NPs using *Mentha pulegium* <sup>6</sup>[48]**

These diffraction patterns are consistent with the standard hematite crystal structure. The sharp, well-defined nature of these peaks suggests high crystallinity of the synthesized nanoparticles. Furthermore, the broadening of diffraction peaks provides information about the crystallite size, which can be quantified using the Scherrer equation or other peak analysis methods.

These XRD findings demonstrate the efficacy of green synthesis methods in producing well-defined, crystalline  $\alpha$ -Fe<sub>2</sub>O<sub>3</sub> NPs. The technique not only confirms the formation of the desired hematite phase but also provides crucial information about the crystallite size and structural properties of the synthesized nanoparticles, validating the success of eco-friendly synthesis protocols.

## 5. Applications of Green-Synthesized $\alpha$ -Fe<sub>2</sub>O<sub>3</sub> Nanoparticles

### 5.1 Photocatalytic Degradation of Environmental Pollutants

The degradation of organic dyes in aqueous environments represents a significant global environmental challenge [49].  $\alpha$ -Fe<sub>2</sub>O<sub>3</sub> NPs have emerged as promising photocatalysts for this application due to their non-toxicity, stability, corrosion resistance, and efficient photocatalytic performance [50]. Photocatalytic degradation, a subset of advanced oxidation processes (AOPs), is highly effective for the decomposition of toxic organic pollutants in water. Figure 6 illustrates the mechanism of this process, which involves the formation of highly reactive hydroxyl radicals ( $\cdot$ OH) in the presence of a semiconductor photocatalyst. Under illumination by UV, visible, or natural solar light, these photocatalysts facilitate the breakdown of organic pollutants into water and carbon dioxide [51]

<sup>6</sup>Reprinted from Science Direct, *Desalin. Water Treat.*, Vol. 317, M. B. Goudjil, H. Dali, S. Zighmi, Z. Mahcene, and S. E. Bencheikh, “Biosynthesis of hematite phase  $\alpha$ -Fe<sub>2</sub>O<sub>3</sub> nanoparticles using an aqueous extract of *Rosmarinus officinalis* leaves”, p. 100079, 2024, with permission from Elsevier, [10.1016/j.dwt.2024.100079](https://doi.org/10.1016/j.dwt.2024.100079)

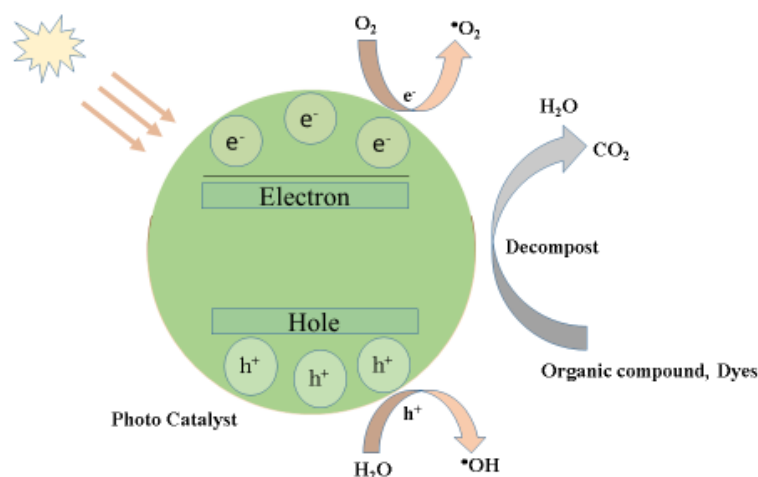


**Figure: 6 Mechanism of Degradation process[51]**

Several studies have demonstrated the efficacy of green-synthesized  $\alpha$ -Fe<sub>2</sub>O<sub>3</sub> NPs in photocatalytic applications:  $\alpha$ -Fe<sub>2</sub>O<sub>3</sub> NPs synthesized using hot water extract of *mandarin* (*Citrus reticulatum*) peels exhibited significant degradation capacity for both anionic and cationic dyes, as well as dichlorophenols, under visible light irradiation [52]. G. K. Weldegebrical and A. K. Sibhatu reported the synthesis of  $\alpha$ -Fe<sub>2</sub>O<sub>3</sub> NPs using *Vernonia amygdalina* leaf extract with Fe(NO<sub>3</sub>)<sub>3</sub>·9H<sub>2</sub>O as a precursor. These NPs demonstrated efficient degradation of Methyl Orange (MO) and Methylene Blue (MB) under sunlight irradiation at alkaline pH, enhanced by the addition of a small amount of H<sub>2</sub>O<sub>2</sub> as an oxidant [53]. Raja Selvaraj et al. synthesized  $\alpha$ -Fe<sub>2</sub>O<sub>3</sub> NPs using *Bridelia retusa* leaf extract, which completely degraded Crystal Violet (CV) via a Fenton-like catalytic degradation process [54].  $\alpha$ -Fe<sub>2</sub>O<sub>3</sub> NPs synthesized using *Aspergillus niger* achieved up to 97% removal efficiency of crystal violet dye within 150 minutes [55]. These  $\alpha$ -Fe<sub>2</sub>O<sub>3</sub> NPs not only enhance environmental remediation efforts but also exhibit antimicrobial properties, rendering them valuable for both wastewater treatment and public health applications. The dual functionality of these nanoparticles highlights their potential as multifaceted solutions for environmental and health challenges. The observed high degradation efficiencies and broad applicability across various dyes underscore the potential of green-synthesized  $\alpha$ -Fe<sub>2</sub>O<sub>3</sub> NPs as environmentally friendly and effective photocatalysts for water treatment applications. Future research directions may include optimizing synthesis parameters for enhanced photocatalytic activity, investigating the degradation mechanisms of different pollutants, and exploring the scalability of these green synthesis methods for industrial applications.

### 5.2 Antimicrobial activity:

The emergence of antimicrobial resistance has necessitated the development of novel antimicrobial agents and the enhancement of existing antibiotic efficacy. In this context, metal and metal oxide nanoparticles, including those of copper oxide, zinc oxide, gold, silver, and iron oxide, have gathered significant attention due to their potential antimicrobial properties.

Green-synthesized silver nanoparticles (AgNPs) have demonstrated notable antimicrobial activity against a broad spectrum of bacteria. Studies have reported effective inhibition of both Gram-positive and Gram-negative bacteria, with inhibition zones ranging from 5.5 mm to over 18 mm, depending on the plant extracts used for synthesis [59–61]. The proposed antibacterial mechanisms include the generation of

reactive oxygen species (ROS) and protein denaturation via  $\text{Ag}^+$  ion release. Biogenic AgNPs are often preferred due to their lower cytotoxicity compared to chemically synthesized counterparts. Iron oxide nanoparticles (IONPs), particularly  $\alpha\text{-Fe}_2\text{O}_3$  NPs, have also shown promising antimicrobial properties [27].

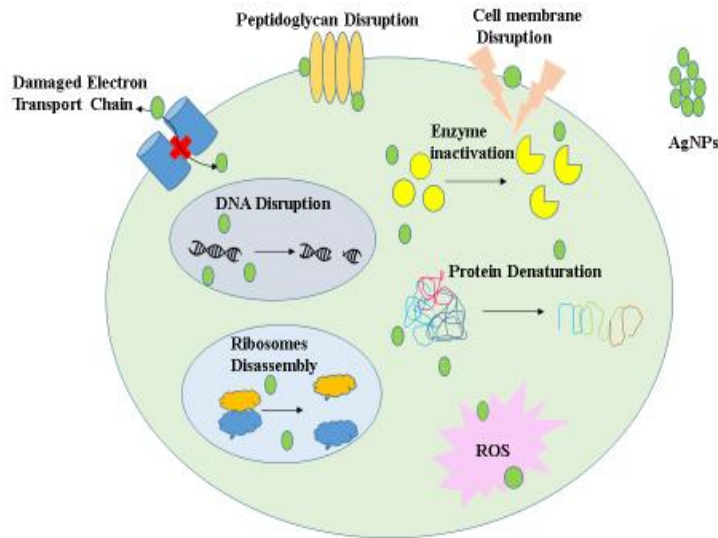


**Figure: 6 Mechanism of antibacterial activity[27]**

$\alpha\text{-Fe}_2\text{O}_3$  NPs synthesized using *Aspergillus niger* exhibited antibacterial effects with minimum inhibitory concentrations (MICs) of 125  $\mu\text{g/mL}$  against *Escherichia coli* (*E.coli*) and 15.62  $\mu\text{g/mL}$  against *Streptococcus mutans* [55]. A study on surface charge effects revealed that positively charged  $\alpha\text{-Fe}_2\text{O}_3$  NPs inhibited *E. coli* growth at concentrations starting from 100 mg/L, while negatively charged variants showed no activity [59]. This highlights the importance of surface properties in antimicrobial efficacy.  $\alpha\text{-Fe}_2\text{O}_3$  NPs derived using *Solanum nigrum* demonstrated effectiveness against both Gram-positive and Gram-negative bacteria, with the highest inhibition observed against *Klebsiella pneumoniae*[60]. Mina Jamzad and Maryam Kamari Bidkorpheh evaluated the antimicrobial activity of  $\alpha\text{-Fe}_2\text{O}_3$  NPs synthesized from aqueous extract of *Laurus nobilis L.* leaves, reporting moderate efficacy against the Gram-positive bacterium *Listeria monocytogenes* [61]

The mechanism of antibacterial activity for these nanoparticles, illustrated in Figure 6, typically involves:

1. Disruption of the bacterial cell membrane
2. Generation of reactive oxygen species (ROS)
3. Interference with cellular metabolic pathways
4. Inhibition of biofilm formation

The diverse antimicrobial activities observed across different green-synthesized  $\alpha\text{-Fe}_2\text{O}_3$  NPs underscore their potential as alternative antimicrobial agents. Their efficacy against both Gram-positive and Gram-negative bacteria coupled with the eco-friendly nature of their synthesis, positions them as promising candidates for biomedical applications, particularly in addressing microbial resistance challenges.

Future research directions should focus on elucidating the precise mechanisms of antimicrobial action, optimizing synthesis protocols for enhanced efficacy, and conducting comprehensive in vivo studies to assess their potential for clinical applications. Additionally, investigating synergistic effects with conventional antibiotics could open new avenues for combating resistant microbial strains.

### 5.3 Anticancer Activity of Green Synthesized $\alpha$ -Fe<sub>2</sub>O<sub>3</sub> Nanoparticles

Recent investigations have shown the anticancer potential of  $\alpha$ -Fe<sub>2</sub>O<sub>3</sub> nanoparticles (NPs). Jumma Yonus et al. reported that  $\alpha$ -Fe<sub>2</sub>O<sub>3</sub> NPs exhibited cytotoxicity against human A-549 lung cancer cells, with 50% cell death observed at various concentrations [23]. Characterization of these NPs revealed needle-like morphology, high surface area, and superparamagnetic properties, which may contribute to their enhanced therapeutic efficacy [45]. In a study by Sania Naz et al.,  $\alpha$ -Fe<sub>2</sub>O<sub>3</sub> NPs demonstrated effective anticancer activity against DU-145 prostate and HL-60 leukemic cell lines. Using an in vitro Sulforhodamine B (SRB) colorimetric cytotoxicity assay, they determined IC<sub>50</sub> values of 12.79 and 11.96  $\mu$ g/mL, respectively [41]. Samar Zuhair et al. investigated the anticancer properties of *Stevia Rebaudiana* L. mediated iron oxide nanoparticles (SRLe- $\alpha$ Fe<sub>2</sub>O<sub>3</sub> NPs) against A549 lung cancer cell lines. While low concentrations of SRLe- $\alpha$ Fe<sub>2</sub>O<sub>3</sub> NPs did not significantly alter cell morphology, higher concentrations resulted in complete cell death. The synthesized NPs exhibited high cytotoxicity, with only 5.4% cell viability after 48 hours of exposure (IC<sub>50</sub> = 51.2  $\mu$ g/mL)[62]. A comprehensive review emphasized the eco-friendly synthesis methods and diverse applications of  $\alpha$ -Fe<sub>2</sub>O<sub>3</sub> NPs, including their potential in cancer treatment [34]. The environmentally friendly synthesis approach not only reduces production costs but also minimizes harmful by-products, making them promising candidates for cancer therapeutic applications [47]

#### Conclusion:

The green synthesis of  $\alpha$ -Fe<sub>2</sub>O<sub>3</sub> NPs has emerged as a promising approach for various applications including wastewater treatment, antimicrobial interventions, and cancer therapeutics. The physicochemical properties of these NPs are significantly influenced by synthesis parameters such as temperature, pH, and precursor concentration. Elevated temperatures generally promote increased particle size due to enhanced diffusion rates, while pH variations affect both size and morphology. Higher precursor concentrations can lead to larger nanoparticles due to increased availability of iron ions for nucleation and growth.

Studies have demonstrated the efficacy of  $\alpha$ -Fe<sub>2</sub>O<sub>3</sub> NPs against both Gram-positive and Gram-negative bacteria with mechanisms involving reactive oxygen species generation. These biogenic nanoparticles exhibit lower cytotoxicity compared to their chemically synthesized counterparts, enhancing their potential for biomedical applications, particularly in addressing antibiotic resistance.

In oncological research,  $\alpha$ -Fe<sub>2</sub>O<sub>3</sub> NPs have shown significant cytotoxicity against various cancer cell lines, including A-549, DU-145, and HL-60, with promising IC<sub>50</sub> values. Characterization of these NPs reveals unique morphological features and superparamagnetic properties, which may contribute to their therapeutic potential. The eco-friendly synthesis methods not only reduce production costs but also minimize harmful by-products, positioning  $\alpha$ -Fe<sub>2</sub>O<sub>3</sub> NPs as viable candidates for cancer treatment applications.

While current studies demonstrate high removal efficiencies for specific dyes and pharmaceuticals in wastewater treatment, further optimization of synthesis parameters is necessary to enhance their effectiveness across diverse environmental conditions. Elucidating the detailed mechanisms underlying their degradation capabilities and biomedical actions is crucial for maximizing their potential in environmental remediation and public health applications.

Future research should focus on:

1. Optimizing synthesis conditions to enhance the efficacy and specificity of  $\alpha$ -Fe<sub>2</sub>O<sub>3</sub> NPs for various applications.
2. Investigating the long-term stability and reusability of these nanoparticles in real-world scenarios to ensure maintained efficacy over time.
3. Conducting comprehensive studies on biocompatibility and potential toxicity to confirm their safety for human health and the environment, particularly in biomedical applications.
4. Exploring the scalability of green synthesis methods for industrial-scale production while maintaining the beneficial properties of the nanoparticles.

The development and application of green-synthesized  $\alpha$ -Fe<sub>2</sub>O<sub>3</sub> NPs align with several United Nations Sustainable Development Goals (SDGs), underscoring their potential impact on global sustainability efforts:

1. SDG 3 (Good Health and Well-being): The antimicrobial and anticancer properties of  $\alpha$ -Fe<sub>2</sub>O<sub>3</sub> NPs contribute to improving health outcomes and combating diseases.
2. SDG 6 (Clean Water and Sanitation): Their application in wastewater treatment supports efforts to improve water quality and increase access to safe, clean water.
3. SDG 9 (Industry, Innovation, and Infrastructure): The green synthesis of  $\alpha$ -Fe<sub>2</sub>O<sub>3</sub> NPs represents an innovative approach to nanomaterial production, promoting sustainable industrialization.
4. SDG 12 (Responsible Consumption and Production): The eco-friendly synthesis methods align with sustainable production practices, reducing waste and minimizing environmental impact.
5. SDG 14 (Life Below Water): By potentially reducing water pollution through effective wastewater treatment, these NPs can contribute to preserving aquatic ecosystems.

In conclusion, green-synthesized  $\alpha$ -Fe<sub>2</sub>O<sub>3</sub> NPs offer a sustainable and efficient approach for addressing environmental and biomedical challenges, while simultaneously supporting key global sustainability objectives. However, further research is essential to fully understand their mechanisms of action, optimize their performance, and ensure their safe application in diverse fields. As we continue to explore and develop these nanoparticles, it is crucial to maintain a focus on their potential to contribute to multiple SDGs, fostering a more sustainable and equitable future.

## References:

1. Tanvir Singh, "Introduction to Nanotechnology System Origin of Nanotechnology," *Tech. Rep.*, no. September, pp. 1–17, 2020, doi: 10.13140/RG.2.2.12770.15049/1.
2. B. Babio, "comprehensive biological assessment and RhB," pp. 7359–7370, 2024, doi: 10.1039/d3ra06354b.
3. M. S. H. Bhuiyan *et al.*, "Green synthesis of iron oxide nanoparticle using Carica papaya leaf extract: application for photocatalytic degradation of remazol yellow RR dye and antibacterial activity," *Heliyon*, vol. 6, no. 8, p. e04603, 2020, doi: 10.1016/j.heliyon.2020.e04603.
4. M. V. Arularasu, J. Devakumar, and T. V. Rajendran, "An innovative approach for green synthesis of iron oxide nanoparticles: Characterization and its photocatalytic activity," *Polyhedron*, vol. 156, pp. 279–290, 2018, doi: 10.1016/j.poly.2018.09.036.
5. B. Cuiping *et al.*, "Removal of rhodamine B by ozone-based advanced oxidation process," *Desalination*, vol. 278, no. 1–3, pp. 84–90, 2011, doi: 10.1016/j.desal.2011.05.009.
6. E. Forgacs, T. Cserhádi, and G. Oros, "Removal of synthetic dyes from wastewaters: A review," *Environ. Int.*, vol. 30, no. 7, pp. 953–971, 2004, doi: 10.1016/j.envint.2004.02.001.

7. J. D. Sachs, G. Lafortune, and G. Fuller, *The SDGs and the UN Summit of the Future. Sustainable Development Report 2024*. 2024. doi: 10.25546/108572.
8. “Water pollution due to textile industry - Textile Magazine, Textile News, Apparel News, Fashion News.”
9. P. Xu *et al.*, “Use of iron oxide nanomaterials in wastewater treatment: A review,” *Sci. Total Environ.*, vol. 424, pp. 1–10, 2012, doi: 10.1016/j.scitotenv.2012.02.023.
10. M. J. Katz, S. C. Riha, N. C. Jeong, A. B. F. Martinson, O. K. Farha, and J. T. Hupp, “Toward solar fuels: Water splitting with sunlight and ‘rust’ ?,” *Coord. Chem. Rev.*, vol. 256, no. 21–22, pp. 2521–2529, 2012, doi: 10.1016/j.ccr.2012.06.017.
11. V. Ramalingam, M. Harshavardhan, and S. Dinesh, “Wet chemical mediated hematite  $\alpha$ -Fe<sub>2</sub>O<sub>3</sub> nanoparticles synthesis: Preparation, characterization and anticancer activity against human metastatic ovarian cancer,” *J. Alloys Compd.*, vol. 834, p. 155118, 2020, doi: 10.1016/j.jallcom.2020.155118.
12. P. Suvaitha, S. Selvam, S. Govindan, B. Perumal, and V. Kandan, “Screening of In Vitro Antibacterial Property of Hematite ( $\alpha$ -Fe<sub>2</sub>O<sub>3</sub>) Nanoparticles: A Green Approach,” *Iran. J. Sci. Technol. Trans. A Sci.*, vol. 0, 2020, doi: 10.1007/s40995-020-00995-0.
13. A. Sajjad, S. Hussain, G. H. Jaffari, S. Hanif, M. N. Qureshi, and M. Zia, “Fabrication of Hematite ( $\alpha$ -Fe<sub>2</sub>O<sub>3</sub>) nanoparticles under different spectral lights transforms physio chemical, biological, and nanozymatic properties,” *Nano Trends*, vol. 2, no. February, p. 100010, 2023, doi: 10.1016/j.nwnano.2023.100010.
14. H. R. Dihom, M. M. Al-Shaibani, R. M. S. Radin Mohamed, A. A. Al-Gheethi, A. Sharma, and M. H. Bin Khamidun, “Photocatalytic degradation of disperse azo dyes in textile wastewater using green zinc oxide nanoparticles synthesized in plant extract: A critical review,” *J. Water Process Eng.*, vol. 47, no. March, p. 102705, 2022, doi: 10.1016/j.jwpe.2022.102705.
15. B. Guldiken, G. Ozkan, G. Catalkaya, F. D. Ceylan, I. Ekin Yalcinkaya, and E. Capanoglu, “Phytochemicals of herbs and spices: Health versus toxicological effects,” *Food Chem. Toxicol.*, vol. 119, pp. 37–49, 2018, doi: 10.1016/j.fct.2018.05.050.
16. L. Soltys, O. Olkhovyy, T. Tatarchuk, and M. Naushad, “Green synthesis of metal and metal oxide nanoparticles: Principles of green chemistry and raw materials,” *Magnetochemistry*, vol. 7, no. 11, 2021, doi: 10.3390/magnetochemistry7110145.
17. A. Rufus, N. Sreeju, V. Vilas, and D. Philip, “Biosynthesis of hematite ( $\alpha$ -Fe<sub>2</sub>O<sub>3</sub>) nanostructures: Size effects on applications in thermal conductivity, catalysis, and antibacterial activity,” *J. Mol. Liq.*, vol. 242, pp. 537–549, 2017, doi: 10.1016/j.molliq.2017.07.057.
18. O. P. Bolade, A. B. Williams, and N. U. Benson, “Green synthesis of iron-based nanomaterials for environmental remediation: A review,” *Environ. Nanotechnology, Monit. Manag.*, vol. 13, p. 100279, 2020, doi: 10.1016/j.enmm.2019.100279.
19. V. V. Makarov *et al.*, “Biosynthesis of stable iron oxide nanoparticles in aqueous extracts of hordeum vulgare and rumex acetosa plants,” *Langmuir*, vol. 30, no. 20, pp. 5982–5988, 2014, doi: 10.1021/la5011924.
20. Priya, Naveen, K. Kaur, and A. K. Sidhu, “Green Synthesis: An Eco-friendly Route for the Synthesis of Iron Oxide Nanoparticles,” *Front. Nanotechnol.*, vol. 3, no. June, 2021, doi: 10.3389/fnano.2021.655062.
21. K. S. Siddiqi, A. ur Rahman, Tajuddin, and A. Husen, “Biogenic Fabrication of Iron/Iron Oxide

- Nanoparticles and Their Application,” *Nanoscale Res. Lett.*, vol. 11, no. 1, 2016, doi: 10.1186/s11671-016-1714-0.
22. Z. Emamifard and H. R. Rajabi, “Green synthesis of hematite nanoparticles using aqueous extract of *Teucrium Polium* after microwave- assisted extraction : synthesis , characterization and evaluation of some biological activities,” *MedBioTech J.*, vol. 5, no. 2, pp. 15–22, 2021.
23. J. Yoonus, R. Resmi, and B. Beena, “Evaluation of antibacterial and anticancer activity of green synthesized iron oxide ( $\alpha$ -Fe<sub>2</sub>O<sub>3</sub>) nanoparticles,” *Mater. Today Proc.*, vol. 46, no. xxxx, pp. 2969–2974, 2020, doi: 10.1016/j.matpr.2020.12.426.
24. M. Haris *et al.*, “Oscillatoria limnetica Mediated Green Synthesis of Iron Oxide (Fe<sub>2</sub>O<sub>3</sub>) Nanoparticles and Their Diverse In Vitro Bioactivities,” *Molecules*, vol. 28, no. 5, 2023, doi: 10.3390/molecules28052091.
25. S. K. Noukelag, C. J. Arendse, and M. Maaza, “Biosynthesis of hematite phase  $\alpha$ -Fe<sub>2</sub>O<sub>3</sub> nanoparticles using an aqueous extract of *Rosmarinus officinalis* leaves,” *Mater. Today Proc.*, vol. 43, pp. 3679–3683, 2020, doi: 10.1016/j.matpr.2020.10.977.
26. W. Ahmad *et al.*, “Eco-benign approach to synthesize spherical iron oxide nanoparticles: A new insight in photocatalytic and biomedical applications,” *J. Photochem. Photobiol. B Biol.*, vol. 205, p. 111821, 2020, doi: 10.1016/j.jphotobiol.2020.111821.
27. S. A. Akintelu, A. K. Oyebamiji, S. C. Olugbeko, and A. S. Folorunso, “Green synthesis of iron oxide nanoparticles for biomedical application and environmental remediation: A review,” *Eclat. Quim.*, vol. 46, no. 4, pp. 17–37, 2021, doi: 10.26850/1678-4618eqj.v46.4.2021.p17-37.
28. J. K. Patra and K. H. Baek, “Green Nanobiotechnology: Factors Affecting Synthesis and Characterization Techniques,” *J. Nanomater.*, vol. 2014, 2014, doi: 10.1155/2014/417305.
29. K. Rajendran and S. Sen, “Optimization of process parameters for the rapid biosynthesis of hematite nanoparticles,” *J. Photochem. Photobiol. B Biol.*, vol. 159, pp. 82–87, 2016, doi: 10.1016/j.jphotobiol.2016.03.023.
30. D. Sharma, L. Ledwani, T. Mehrotra, N. Kumar, N. Pervaiz, and R. Kumar, “Biosynthesis of hematite nanoparticles using *Rheum emodi* and their antimicrobial and anticancerous effects in vitro,” *J. Photochem. Photobiol. B Biol.*, vol. 206, p. 111841, 2020, doi: 10.1016/j.jphotobiol.2020.111841.
31. J. A. A. Abdullah, Á. Díaz-García, J. Y. Law, A. Romero, V. Franco, and A. Guerrero, “Sustainable Nanomagnetism: Investigating the Influence of Green Synthesis and pH on Iron Oxide Nanoparticles for Enhanced Biomedical Applications,” *Polymers (Basel)*, vol. 15, no. 18, 2023, doi: 10.3390/polym15183850.
32. J. A. A. Abdullah, L. Salah Eddine, B. Abderrhmane, M. Alonso-González, A. Guerrero, and A. Romero, “Green synthesis and characterization of iron oxide nanoparticles by *Phoenix dactylifera* leaf extract and evaluation of their antioxidant activity,” *Sustain. Chem. Pharm.*, vol. 17, no. April, 2020, doi: 10.1016/j.scp.2020.100280.
33. S. C. Kumari, V. Dhand, and P. N. Padma, “Green synthesis of metallic nanoparticles: a review,” *Nanomater. Appl. Biofuels Bioenergy Prod. Syst.*, pp. 259–281, 2021, doi: 10.1016/B978-0-12-822401-4.00022-2.
34. M. F. Al-Hakkani, G. A. Gouda, and S. H. A. Hassan, “A review of green methods for phyto-fabrication of hematite ( $\alpha$ -Fe<sub>2</sub>O<sub>3</sub>) nanoparticles and their characterization, properties, and applications,” *Heliyon*, vol. 7, no. 1, p. e05806, 2021, doi: 10.1016/j.heliyon.2020.e05806.
35. A. Hussain *et al.*, “Synthesis , characterization , and applications of iron oxide nanoparticles,” vol. 17,

no. 4, 2023.

36. N. Basavegowda, K. Mishra, and Y. R. Lee, "Synthesis, characterization, and catalytic applications of hematite ( $\alpha$ -Fe<sub>2</sub>O<sub>3</sub>) nanoparticles as reusable nanocatalyst," *Adv. Nat. Sci. Nanosci. Nanotechnol.*, vol. 8, no. 2, 2017, doi: 10.1088/2043-6254/aa6885.
37. M. Farahmandjou, "CHEMISTRY," no. April, 2015, doi: 10.22036/pcr.2015.9193.
38. A. Ahmed, M. Usman, B. Yu, Y. Shen, and H. Cong, "Sustainable fabrication of hematite ( $\alpha$ -Fe<sub>2</sub>O<sub>3</sub>) nanoparticles using biomolecules of Punica granatum seed extract for unconventional solar-light-driven photocatalytic remediation of organic dyes," *J. Mol. Liq.*, vol. 339, p. 116729, 2021, doi: 10.1016/j.molliq.2021.116729.
39. K. Akhtar, S. A. Khan, S. B. Khan, and A. M. Asiri, *Scanning electron microscopy: Principle and applications in nanomaterials characterization*. 2018. doi: 10.1007/978-3-319-92955-2\_4.
40. N. Raval, R. Maheshwari, D. Kalyane, S. R. Youngren-Ortiz, M. B. Chougule, and R. K. Tekade, *Importance of physicochemical characterization of nanoparticles in pharmaceutical product development*. Elsevier Inc., 2018. doi: 10.1016/B978-0-12-817909-3.00010-8.
41. S. Naz, M. Islam, S. Tabassum, N. F. Fernandes, E. J. Carcache de Blanco, and M. Zia, "Green synthesis of hematite ( $\alpha$ -Fe<sub>2</sub>O<sub>3</sub>) nanoparticles using Rhus punjabensis extract and their biomedical prospect in pathogenic diseases and cancer," *J. Mol. Struct.*, vol. 1185, pp. 1–7, 2019, doi: 10.1016/j.molstruc.2019.02.088.
42. A. Dehbi, Y. Dehmani, H. Omari, A. Lammini, K. Elazhari, and A. Abdallaoui, "Hematite iron oxide nanoparticles ( $\alpha$ -Fe<sub>2</sub>O<sub>3</sub>): Synthesis and modelling adsorption of malachite green," *J. Environ. Chem. Eng.*, vol. 8, no. 1, p. 103394, 2020, doi: 10.1016/j.jece.2019.103394.
43. P. N. V. K. Pallela *et al.*, "Antibacterial efficacy of green synthesized  $\alpha$ -Fe<sub>2</sub>O<sub>3</sub> nanoparticles using Sida cordifolia plant extract," *Heliyon*, vol. 5, no. 11, p. e02765, 2019, doi: 10.1016/j.heliyon.2019.e02765.
44. H. Y. El-Kassas, M. A. Aly-Eldeen, and S. M. Gharib, "Green synthesis of iron oxide (Fe<sub>3</sub>O<sub>4</sub>) nanoparticles using two selected brown seaweeds: Characterization and application for lead bioremediation," *Acta Oceanol. Sin.*, vol. 35, no. 8, pp. 89–98, 2016, doi: 10.1007/s13131-016-0880-3.
45. N. Ndou, T. Rakgotho, M. Nkuna, I. Z. Doumbia, T. Mulaudzi, and R. F. Ajayi, "Green Synthesis of Iron Oxide (Hematite) Nanoparticles and Their Influence on Sorghum bicolor Growth under Drought Stress," *Plants*, vol. 12, no. 7, pp. 1–23, 2023, doi: 10.3390/plants12071425.
46. M. Nasrollahzadeh, M. Atarod, M. Sajjadi, S. M. Sajadi, and Z. Issaabadi, *Plant-Mediated Green Synthesis of Nanostructures: Mechanisms, Characterization, and Applications*, 1st ed., vol. 28. Elsevier Ltd., 2019. doi: 10.1016/B978-0-12-813586-0.00006-7.
47. M. S. Aida, N. Alonizan, B. Zarrad, and M. Hjiri, "Green synthesis of iron oxide nanoparticles using Hibiscus plant extract," *J. Taibah Univ. Sci.*, vol. 17, no. 1, 2023, doi: 10.1080/16583655.2023.2221827.
48. M. B. Goudjil, H. Dali, S. Zighmi, Z. Mahcene, and S. E. Bencheikh, "Photocatalytic degradation of methylene blue dye with biosynthesized Hematite  $\alpha$ -Fe<sub>2</sub>O<sub>3</sub> nanoparticles under UV-Irradiation," *Desalin. Water Treat.*, vol. 317, no. August 2023, p. 100079, 2024, doi: 10.1016/j.dwt.2024.100079.
49. J. Fowsiya, G. Madhumitha, N. A. Al-Dhabi, and M. V. Arasu, "Photocatalytic degradation of Congo red using Carissa edulis extract capped zinc oxide nanoparticles," *J. Photochem. Photobiol. B Biol.*, vol. 162, pp. 395–401, 2016, doi: 10.1016/j.jphotobiol.2016.07.011.

50. E. A. Abdelrahman, R. M. Hegazey, Y. H. Kotp, and A. Alharbi, "Facile synthesis of Fe<sub>2</sub>O<sub>3</sub> nanoparticles from Egyptian insecticide cans for efficient photocatalytic degradation of methylene blue and crystal violet dyes," *Spectrochim. Acta - Part A Mol. Biomol. Spectrosc.*, vol. 222, p. 117195, 2019, doi: 10.1016/j.saa.2019.117195.
51. J. P. Shubha, K. Kavalli, S. F. Adil, M. E. Assal, M. R. Hatshan, and N. Dubasi, "Facile green synthesis of semiconductive ZnO nanoparticles for photocatalytic degradation of dyes from the textile industry: A kinetic approach," *J. King Saud Univ. - Sci.*, vol. 34, no. 5, p. 102047, 2022, doi: 10.1016/j.jksus.2022.102047.
52. H. R. Ali, H. N. Nassar, and N. S. El-Gendy, "Green synthesis of  $\alpha$ -Fe<sub>2</sub>O<sub>3</sub> using Citrus reticulum peels extract and water decontamination from different organic pollutants," *Energy Sources, Part A Recover. Util. Environ. Eff.*, vol. 39, no. 13, pp. 1425–1434, 2017, doi: 10.1080/15567036.2017.1336818.
53. G. Kassegn and A. Kassegn, "Optik Photocatalytic activity of biosynthesized  $\alpha$ -Fe<sub>2</sub>O<sub>3</sub> nanoparticles for the degradation of methylene blue and methyl orange dyes," vol. 241, no. May, pp. 1–15, 2021.
54. R. Selvaraj *et al.*, "Green synthesis of magnetic  $\alpha$ -Fe<sub>2</sub>O<sub>3</sub> nanospheres using Bridelia retusa leaf extract for Fenton-like degradation of crystal violet dye," *Appl. Nanosci.*, vol. 11, no. 8, pp. 2227–2234, 2021, doi: 10.1007/s13204-021-01952-y.
55. E. Saied, S. S. Salem, A. A. Al-Askar, F. M. Elkady, A. A. Arishi, and A. H. Hashem, "Mycosynthesis of Hematite ( $\alpha$ -Fe<sub>2</sub>O<sub>3</sub>) Nanoparticles Using Aspergillus niger and Their Antimicrobial and Photocatalytic Activities," *Bioengineering*, vol. 9, no. 8, 2022, doi: 10.3390/bioengineering9080397.
56. E. Urnukhsaikhon, B. E. Bold, A. Gunbileg, N. Sukhbaatar, and T. Mishig-Ochir, "Antibacterial activity and characteristics of silver nanoparticles biosynthesized from Carduus crispus," *Sci. Rep.*, vol. 11, no. 1, pp. 1–12, 2021, doi: 10.1038/s41598-021-00520-2.
57. X. Xin, C. Qi, L. Xu, Q. Gao, and X. Liu, "Green synthesis of silver nanoparticles and their antibacterial effects," *Front. Chem. Eng.*, vol. 4, no. August, pp. 1–18, 2022, doi: 10.3389/fceng.2022.941240.
58. D. Garibo *et al.*, "Green synthesis of silver nanoparticles using Lysiloma acapulcensis exhibit high-antimicrobial activity," *Sci. Rep.*, vol. 10, no. 1, pp. 1–11, 2020, doi: 10.1038/s41598-020-69606-7.
59. S. Vihodceva *et al.*, "Antibacterial activity of positively and negatively charged hematite ( $\alpha$ -Fe<sub>2</sub>O<sub>3</sub>) nanoparticles to escherichia coli, staphylococcus aureus and vibrio fischeri," *Nanomaterials*, vol. 11, no. 3, pp. 1–26, 2021, doi: 10.3390/nano11030652.
60. S. Hayet, K. M. Sujana, A. Mustari, and M. A. Miah, "Hemato-biochemical profile of turkey birds selected from Sherpur district of Bangladesh," *Int. J. Adv. Res. Biol. Sci.*, vol. 8, no. 6, pp. 1–5, 2021, doi: 10.22192/ijarbs.
61. M. Jamzad and M. Kamari Bidkorpeh, "Green synthesis of iron oxide nanoparticles by the aqueous extract of Laurus nobilis L. leaves and evaluation of the antimicrobial activity," *J. Nanostructure Chem.*, vol. 10, no. 3, pp. 193–201, 2020, doi: 10.1007/s40097-020-00341-1.
62. S. Z. Alshawwa *et al.*, "In Situ Biosynthesis of Reduced Alpha Hematite ( $\alpha$ -Fe<sub>2</sub>O<sub>3</sub>) Nanoparticles by Stevia Rebaudiana L. Leaf Extract: Insights into Antioxidant, Antimicrobial, and Anticancer Properties," *Antibiotics*, vol. 11, no. 9, 2022, doi: 10.3390/antibiotics11091252.